Molecular Cancer Therapeutics

# A Novel Photodynamic Therapy Targeting Cancer Cells and Tumor-Associated Macrophages

Noriyuki Hayashi[1], Hiromi Kataoka[1], Shigenobu Yano[2,3], Mamoru Tanaka[1], Kazuhiro Moriwaki[4], Haruo Akashi[4], Shugo Suzuki[5], Yoshinori Mori[1], Eiji Kubota[1], Satoshi Tanida[1], Satoru Takahashi[5], and Takashi Joh[1]

## Abstract

Tumor-associated macrophages (TAM) in cancer stroma play important roles for cancer cell growth, invasion, angiogenesis, and metastases. We synthesized a novel photosensitizer, mannose-conjugated chlorin (M-chlorin), designed to bind mannose receptors highly expressed on TAMs. We evaluated the newly available photodynamic therapy (PDT) with M-chlorin against gastric and colon cancer. We evaluated PDT with M-chlorin for *in vitro* cytotoxicity and apoptosis induction in cancer cells compared with chlorin alone and glucose-conjugated chlorin (G-chlorin). The subcellular localization of M-chlorin was observed by confocal microscopy, and the M-chlorin PDT effects against TAMs including THP-1–induced M2-polarized macrophages were evaluated. Anticancer effects were also investigated in an allograft model where cytotoxic effects against TAMs in the cancer cell stroma were analyzed by immunohistochemistry. M-chlorin PDT strongly induced cell death in cancer cells to almost the same extent as G-chlorin PDT by inducing apoptosis. M-chlorin was incorporated into cancer cells where it localized mainly in lysosomes and endoplasmic reticula. M-chlorin PDT revealed strong cytotoxicity for M2 macrophages induced from THP-1 cell lines, and it induced stronger cytotoxicity than G-chlorin PDT in the allograft model through killing both cancer cells and TAMs in the cancer stroma. The M-chlorin PDT produced strong cytotoxicity against cancer tissue by inducing apoptosis of both cancer cells and TAMs in the cancer stroma. This novel PDT thus stands as a new candidate for very effective, next-generation PDT. *Mol Cancer Ther; 14(2); 452–60. ©2014 AACR.*



## Introduction

Tumor stroma consists of activated fibroblasts, myofibroblasts, smooth muscle cells, endothelial cells, and inflammatory cells, including macrophages (1–5). Macrophages are often the most abundant immune cells in the tumor microenvironment and are key regulators of the inflammatory process during cancer. Macrophages migrating to tumor stroma are called tumor-associated macrophages (TAM; refs. 6–9). TAMs play several M2-associated protumoral roles during the cancer process including in tumor cell growth, angiogenesis, matrix remodeling, and metastases. Indeed, the abundance of TAMs has been correlated with poor prognosis in various types of human cancers (10–14).

TAMs are known to specifically express abundant levels of CD206, a mannose receptor (15–17), which is also called the "pattern-recognition receptor." These receptors are crucial for the macrophage's role in engulfing invading organisms and degrading them through endocytosis and phagocytosis (18, 19).

Recently, TAMs have been investigated as novel therapeutic targets of cancer therapy (20–24). However, the therapies being trialed kill not only TAMs in cancer stroma, but also other M2 macrophages throughout the body that are important for normal processes including parasite containment, promotion of tissue remodeling, and immune regulation. Thus, targeting M2 macrophages systemically carries the risk of inducing an immunocompromised state (7, 25, 26).

Photodynamic therapy (PDT) is now an established treatment for cancer and some nonmalignant diseases (27). PDT uses the combination of nontoxic dyes or photosensitizers and harmless visible light to produce reactive oxygen species (ROS) and destroy tumors (28, 29). The anticancer effects of PDT are consequences of a low-to-moderately selective degree of photosensitizer uptake by malignant cells, direct cytotoxicity of ROS produced by photosensitizer and irradiation, and severe tumor vascular damage that impairs blood supply to the treated area (30–32). Importantly, these biologic effects of PDT are limited to the particular areas of tissues exposed to light.

PDT using porfimer sodium, a first-generation photosensitizer used clinically in Japan, has disadvantages such as the requirement for shielding from light for 4 to 6 weeks and a high incidence of skin toxicity due to the photosensitivity of porfimer sodium

[1]Department of Gastroenterology and Metabolism, Nagoya City University Graduate School of Medical Sciences, Mizuho-cho, Mizuho-ku, Nagoya, Japan. [2]Graduate School of Materials Science, Nara Institute of Science and Technology, Ikoma, Nara, Japan. [3]Office of Society-Academia Collaboration for Innovation, Kyoto University, Katsura, Nishikyo-ku, Kyoto, Japan. [4]Reseach Institute of Natural Sciences, Okayama University of Science, Kita-ku, Okayama-shi, Okayama, Japan. [5]Department of Experimental Pathology and Tumor Biology, Nagoya City University Graduate School of Medical Sciences, Mizuho-cho, Mizuho-ku, Nagoya, Japan.

**Note:** Supplementary data for this article are available at Molecular Cancer Therapeutics Online (http://mct.aacrjournals.org/).

**Corresponding Author:** Hiromi Kataoka, Department of Gastroenterology and Metabolism, Nagoya City University Graduate School of Medical Sciences, 1 Kawasumi, Mizuho-cho, Mizuho-ku, Nagoya 467-8601, Japan. Phone: 81-52-853-8211; Fax: 81-52-852-0952; E-mail: hkataoka@med.nagoya-cu.ac.jp

**doi:** 10.1158/1535-7163.MCT-14-0348

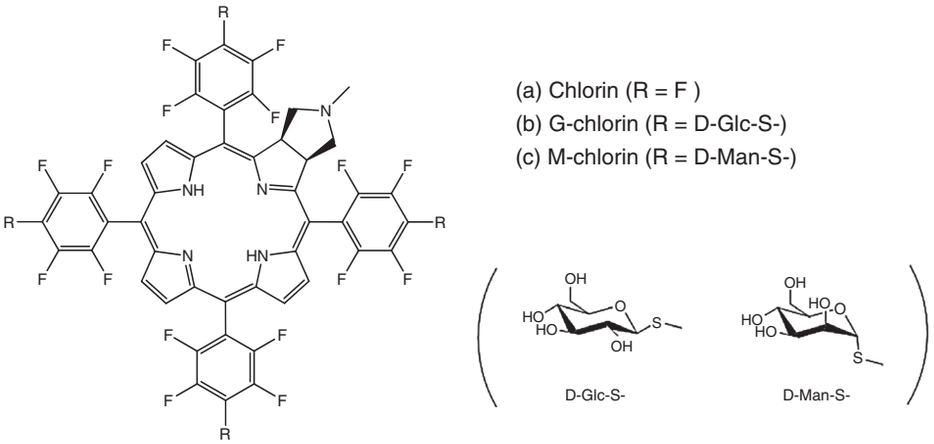


**Figure 1.**
Chemical structure of $H_2$TFPC-SMan. The structures of 5, 10, 15, 20-tetrakis (pentafluorophenyl)-2, 3-(methano [N-methyl] iminomethano) chlorin: chlorin ($H_2$TFPC), 5, 10, 15, 20-tetrakis (4-(β-D-glucopyranosylthio)-2, 3, 5, 6-tetrafluorophenyl)-2, 3-(methano [N-methyl] iminomethano) chlorin: G-chlorin (H2TFPC-SGlc) and 5, 10, 15, 20-tetrakis (4-(a-D-mannopyranosylthio)-2, 3, 5, 6-tetrafluorophenyl)-2, 3-(methano [*N*-methyl] iminomethano) chlorin: M-chlorin ($H_2$TFPC-SMan) are shown.

(33, 34). PDT with talaporfin, a second-generation photosensitizer, involves a shorter period of light shielding (about 2 weeks) and lower incidence of skin toxicity than PDT with porfimer sodium, and the wavelength of laser light used for talaporfin (664 nm) is longer than that needed to excite porfimer sodium (630 nm); thus, the talaporfin PDT effects may penetrate deeper into the tissue (33, 35). To improve the efficacy of PDT, photosensitizers with better cancer cell specificity and selectivity are needed. In our previous study, we reported that PDT using the newly developed photosensitizer, glucose-conjugated chlorin (G-chlorin), exerted approximately 30 times more cytotoxicity than talaporfin PDT (36). Cancer cells incorporate more glucose than normal cells in a phenomenon known as the Warburg effect (37), and we utilized this phenomenon for PDT like it is used diagnostically in fluorodeoxyglucose positron emission tomography/computed tomography (38–40). Accordingly, using a glucose-conjugated photosensitizer increased the cancer cell selectivity and specificity of PDT (36, 41).

On the basis of our previous study and other reports, we then proposed targeting TAMs using PDT to block cancer development. In this study, we examined antitumor effects by using newly synthesized mannose-conjugated chlorin (M-chlorin) to target mannose receptors on TAMs. This PDT approach is the first therapy to target only TAMs in cancer stroma without any systemic damage to M2 macrophages.

## Materials and Methods

### Photosensitizers

M-chlorin ($H_2$TFPC-SMan, 5, 10, 15, 20-tetrakis (4-(α-D-mannopyranosylthio)-2, 3, 5, 6-tetrafluorophenyl)-2, 3-(methano (N-methyl) iminomethano) chlorin), G-chlorin ($H_2$TFPC-SGlc, 5, 10, 15, 20-tetrakis (4-(β-D-glucopyranosylthio)-2, 3, 5, 6-tetrafluorophenyl)-2, 3-(methano (*N*-methyl) iminomethano) chlorin), and chlorin ($H_2$TFPC, 5, 10, 15, 20-tetrakis (2, 3, 4, 5, 6-pentafluorophenyl)-2, 3-(methano(*N*-methyl)iminomethano) chlorin) were synthesized and provided by the laboratory of the Kyoto University (Kyoto, Japan) and Okayama University of Science (Okayama, Japan; ref. 42) and characterized by mass spectroscopy and elemental analyses (Fig. 1).

### Cell culture

The human gastric cancer cell lines MKN28 (No.0253; Japanese Cancer Research Resources Bank) and MKN45 (No.0254; Japanese Cancer Research Resources Bank) were cultured in RPMI1640 (Sigma-Aldrich) supplemented with 10% FBS, 100 U/mL penicillin,100 μg/mL streptomycin, and 0.25 μg/mL amphotericin B. The human colon cancer cell lines HT29 (No. HTB-38, ATCC) and HCT116 (No.CCL-274, ATCC) were cultured in McCoy 5A Medium (Sigma-Aldrich) supplemented with 10% FBS, 100 U/mL penicillin, 100 μg/mL streptomycin, and 0.25 μg/mL amphotericin B. The murine colorectal cancer cell line CT26 (No.CRL-2638, ATCC) was cultured in DMEM (Sigma-Aldrich) supplemented with 10% FBS, 100 U/mL penicillin, 100 μg/mL streptomycin, and 0.25 μg/mL amphotericin B. The human monocyte cell line THP-1 (ATCC TIB202; ATCC) was cultured in RPMI1640 supplemented with 10% FBS, 100 U/mL penicillin, 100 μg/mL streptomycin, and 0.25 μg/mL amphotericin B and 0.05 mmol/L 2-mercaptoethanol. Cells were cultured under an atmosphere of 5% $CO_2$ at 37°C.

To generate M1-polarized THP-1 macrophages, THP-1 cells were treated with 320 nmol/L phorbyl myristate acetate (PMA) for 6 hours and cultured with PMA plus 20 ng/mL INFγ and 100 ng/mL lipopolysaccharide for 18 hours. To generate M2-polarized THP-1 macrophages, THP-1 cells were treated with 320 nmol/L PMA for 6 hours and cultured with PMA plus 20 ng/mL IL4 and 20 ng/mL IL13 for 18 hours (43).

Cell authentication (STR profile) was performed to all human cancer cell lines (MKN28, MKN45, HT29, HCT116, and THP-1) by JCRB cell bank on February 25, 2014.

### *In vitro* PDT

The gastric and colon cancer cells (MKN28, MKN45, HT29, HCT116, CT26) and M1, M2-polarized THP-1 macrophages were incubated with photosensitizer in culture medium for 24 hours. Cancer cells and macrophages were washed once in PBS, covered with PBS, and irradiated at 13.9 and 5.6 J/cm$^2$ (intensity: 30.8 mW/cm$^2$) of LED light (Opto Code Corporation), which emits 660 nm wavelength.

### Cell viability assay

Cell viability was determined using a WST-8 cell proliferation assay (Dojindo). Gastric and colon cancer cells and macrophages were seeded into 96-well culture plates at $5 \times 10^3$ cells/100 μL/well and incubated overnight. Cells were then incubated with photosensitizers at 37°C for 24 hours, irradiated, and incubated with culture medium for a further 24 hours. To determine survival, cells were incubated with cell counting kit-8 for 4 hours and

absorption at 450 nm was measured with a microplate reader (SPECTRA MAX340, Molecular Devices). Cell viability was expressed as a percentage of treated cells versus untreated control cells. The half maximal (50%) inhibitory concentration ($IC_{50}$) was calculated.

### Caspase-3/7 assay

Apoptosis in the CT26 cells was assessed using the Caspase-Glo3/7 Assay Kit (Promega) according to the manufacturer's instructions. CT26 cells were seeded into 96-well culture plates and incubated overnight. Cells were then incubated with 0.2 μmol/L photosensitizers at 37°C for 24 hours and irradiated. Analyses were performed at 0, 1, 4, 8, and 12 hours after PDT by adding 50 μL of caspase-3/7 reagent to each well, mixing, and incubating for 1 hour at room temperature. Luminescence was measured using a Lu mat LB 9507 instrument (EG&G BERTHOLD). Caspase-3/7 activity was expressed as percentage of the untreated control.

### Intracellular localization of photosensitizers

CT26 cells were seeded into 24-well culture plates and incubated overnight. Cells were incubated with 0.2 μmol/L M-chlorin for 24 hours and stained with organelle-specific fluorescent probes, as follows: lysosomes with 0.1 μmol/L LysoTracker Green (Invitrogen) at 37°C for 30 minutes; mitochondria with 0.1 μmol/L MitoTracker Green FM (Invitrogen) at 37°C for 10 minutes; Golgi with 5 μmol/L NBD C6-ceramide at 4°C for 30 minutes; and endoplasmic reticulum with 0.1 μmol/L ER-Tracker Green (Invitrogen) at 37°C for 30 minutes. Following incubation, cells were rinsed with PBS to remove free dyes, and the stained cells were observed live by confocal laser microscopy (Nikon A1 confocal system Nikon Instech Co., Ltd.) and data were analyzed using NIS element imaging software (Nikon). Band-pass emission filters of 505 to 530 nm and 650 nm were used.

### Real-time reverse transcription PCR

CD68, CD206, TNFα, and GAPDH mRNA expression in THP-1 and M1, M2-polarized THP-1 macrophages was measured by real-time reverse transcription PCR (RT-PCR). GAPDH was chosen as an endogenous control to normalize the expression data. mRNA was reverse transcribed into complementary DNA (cDNA) using a High-Capacity cDNA Reverse Transcription Kit (Applied Biosystems) according to the manufacturer's instructions. TaqMan gene expression assays for CD68 (Hs02836816_g1), CD206 (Hs00267207_m1), TNFα (Hs01113624_g1), and GAPDH (Hs99999905_m1) were purchased from Applied Biosystems, and quantitative RT-PCR analyses were performed in triplicate using an ABI 7500 Fast Real-Time PCR system (Applied Biosystems) according to the supplier's recommendations. All data are presented as fold changes of internal control.

### Animals and tumor models

Female mice (BALB/c CrSlc) ages 4 weeks and weighing 20 to 25 g were obtained from Japan SLC. Animals were allowed to acclimatize for 2 weeks in the animal facility before any interventions were initiated. Allograft tumor models were established by implanting $1 \times 10^6$ colon cancer cells (CT26) subcutaneously under the right flank of BALB/c mice. The procedures in these experiments were approved by the Nagoya City University Center for Experimental Animal Science, and mice were raised according to the Nagoya City University for Animal Experiments.

### *In vivo* PDT

When transplanted tumors grew to approximately 100 $mm^3$, mice were given an intraperitoneal injection of photosensitizer (chlorin, G-chlorin, M-chlorin) at a dose of 6.25 μmol/kg. At 24 hours after injection, tumors were irradiated with 660 nm LED at a dose of 13.9 $J/cm^2$. Irradiation was repeated twice on day 1 and day 8. Tumor growth was monitored by measuring tumor volume with vernier calipers, and calculated using the following formula: (length × width × width). Relative tumor growth was assessed by comparing tumor volume with that measured on day 1. Treated groups and control groups consisted of 5 mice and 4 mice, respectively. All *in vivo* assays were performed three times.

### Immunohistochemistry of transplanted tumor

After treatment and *in vivo* measurements, the mice were deeply anesthetized and sacrificed at 3 days after the first irradiation (day 4). The tumors were immediately excised and were fixed in formalin for immunohistochemical examination. Anti-F4/80 antibody (ab6640 Abcam) was used as a specific marker for macrophages, and anti-CD206 antibody (MCA2235T A Bio-Rad) was used as a specific marker for TAMs.

Consecutive tissue sections (4 μm thick) were deparaffinized in xylene and hydrated through a graded series of ethanol. After inhibition of endogenous peroxidase activity by immersion in 0.3% $H_2O_2$ methanol solution, sections were incubated with the primary antibody, washed thoroughly in PBS, and then incubated with biotinylated secondary antibody followed by the avidin–biotinylated horseradish peroxidase complex. Finally, immune complexes were visualized by incubation with 0.01% $H_2O_2$ and 0.05% 3,3′-diaminobenzidine tetrachloride (DAB). Nuclear counterstaining was accomplished with Mayer's hematoxylin. Mouse macrophages and TAMs in a 250 × 250 μm area were counted in random triplicates of area from each mouse, and averaged.

### Spectrometer analysis

The accumulation of photosensitizers in the allograft tumors was examined using a semiconductor laser with a VLD-M1 spectrometer (M&M Co., Ltd.) that emitted a laser light with a peak wavelength of 405 ± 1 nm and a light output of 140 mW. The spectrometer and its accessory software (BW-Spec V3. 24; B&W

**Table 1.** The $IC_{50}$ for gastric and colon cancer cells by chlorin, G-chlorin, and M-chlorin PDT

| | Gastric cancer | | Colon cancer | | |
|---|---|---|---|---|---|
| | MKN28 | MKN45 | HT29 | HCT116 | CT26 |
| Chlorin | 2.94 | 3.77 | 3.46 | 4.00 | 0.80 |
| G-chlorin | 0.20 | 0.16 | 0.26 | 0.09 | 0.05 |
| M-chlorin | 0.15 | 0.27 | 0.29 | 0.10 | 0.04 |

NOTE: Gastric and colon cancer cells (MKN28, MKN45, HT29, HCT116, and CT26) were incubated with various concentrations of photosensitizer in culture medium for 24 hours, irradiated with 13.9 $J/cm^2$ of 660 nm LED light, and incubated for 24 hours. Cell viability was determined by a WST-8 assay and expressed by 50% inhibitory concentration ($IC_{50}$). Data are means of five independent experiments.

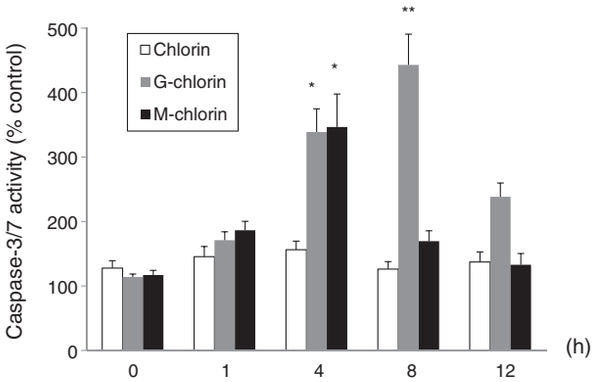


**Figure 2.**
Caspase-3/7 activity in CT26 cells after PDT. CT26 cells were incubated with 0.2 μmol/L photosensitizers (chlorin, G-chlorin, M-chlorin) or negative control, and irradiated with 13.9 J/cm$^2$ of 660 nm LED light. Analyses were performed at 0, 1, 4, 8, and 12 hours after PDT. Caspase-3/7 activity was determined by the Caspase-Glo3/7 Assay and expressed as percentages of the untreated control. Data are means ± SE of six independent experiments. *, $P < 0.05$, G-chlorin and M-chlorin at 0 hour versus G-chlorin and M-chlorin at 4 hours; **, $P < 0.01$, G-chlorin at 0 hour versus G-chlorin at 8 hours.

TEK, Inc.) were used to analyze the spectrum waveform and revealed an amplitude peak (relative fluorescent intensity) at 505 nm for autofluorescence, at 655 nm for photosensitizers. The relative intensities of the photosensitizers were measured by the spectrometer. To reduce measurement error, the relative fluorescence intensity ratios of photosensitizers in the target tissue, which were calculated by dividing the relative fluorescence intensity by that of autofluorescence, were compared.

### Statistical analysis

The statistical significance of differences was determined using the Student *t* test or the Tukey–Kramer method. Differences were considered statistically significant at $P < 0.05$. Data are expressed as means ± SE.

## Results

### PDT with M-chlorin induced cell death in gastric and colon cancer cell lines similarly to that induced by PDT with G-chlorin

We first evaluated the cell death induced by PDT with M-chlorin. Cells were loaded with photosensitizer (chlorin, G-chlorin, M-chlorin) for 24 hours, irradiated with 660 nm LED light at 13.9 J/cm$^2$, and incubated for 24 hours. We then determined the $IC_{50}$ at 24 hours after PDT. As shown in Table 1 and Supplementary Fig. S1, PDT with M-chlorin and G-chlorin induced cell death with 10 to 40 times more cytotoxicity to all cancer cells than chlorin alone. PDT with M-chlorin and G-chlorin were equally effective at killing cancer cells.

### PDT with M-chlorin induced apoptosis

We next investigated the level of apoptosis induced by M-chlorin–mediated PDT. Cells were incubated with 0.2 μmol/L photosensitizers (chlorin, G-chlorin, M-chlorin) for 24 hours, followed by irradiation with 660 nm (13.9 J/cm$^2$), and measurement of caspase-3/7 activity at 0, 1, 4, 8, and 12 hours after PDT. As shown in Fig. 2, PDT with G-chlorin and M-chlorin induced apoptosis from 1 hour after irradiation, with the maximal effects found at 8 hours with G-chlorin and at 4 hours with M-chlorin. PDT with chlorin alone did not activate caspase-3/7 significantly.

### M-chlorin was incorporated into cancer cells and mainly localized in lysosomes and endoplasmic reticula

Next, we investigated the subcellular localization of M-chlorin by confocal microscopy using fluorescence probes for intracellular organelles. Cells were loaded with M-chlorin and incubated with MitoTracker Green, LysoTracker Green, NBD C6 ceramide Green, or ERTracker Green to label mitochondria, lysosomes, Golgi, or endoplasmic reticula, respectively. M-chlorin tended to colocalize with LysoTracker and ERTracker, indicating accumulation in lysosomes and endoplasmic reticula (Fig. 3). On the other hand, G-chlorin seemed to colocalize with MitoTracker, indicating accumulation in mitochondria (Supplementary Fig. S2).

### PDT with M-chlorin strongly induced cell death in M2 macrophages

M1, M2-polarized THP-1 macrophages (CD68 positive) were generated as described previously (43), and compared with THP-1 cells. As shown in Fig. 4A, M1- and M2-polarized THP-1 macrophages expressed significantly higher CD68 than undifferentiated THP-1 macrophages ($P < 0.01$). The M2-polarized THP-1 macrophages also expressed significantly higher mannose receptor

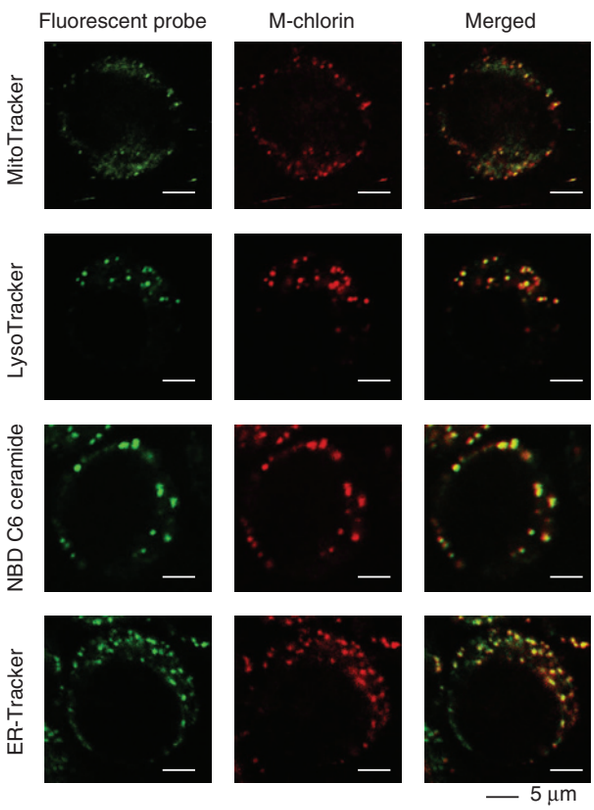


**Figure 3.**
Subcellular localization of M-chlorin. CT26 cells were loaded with M-chlorin for 24 hours and labeled with Mito Tracker Green, Lyso Tracker Green, NBD C6 ceramide Green, or ER Tracker Green. The images were obtained by confocal microscopy (Original magnification, × 1,000; scale bar, 5 μm).

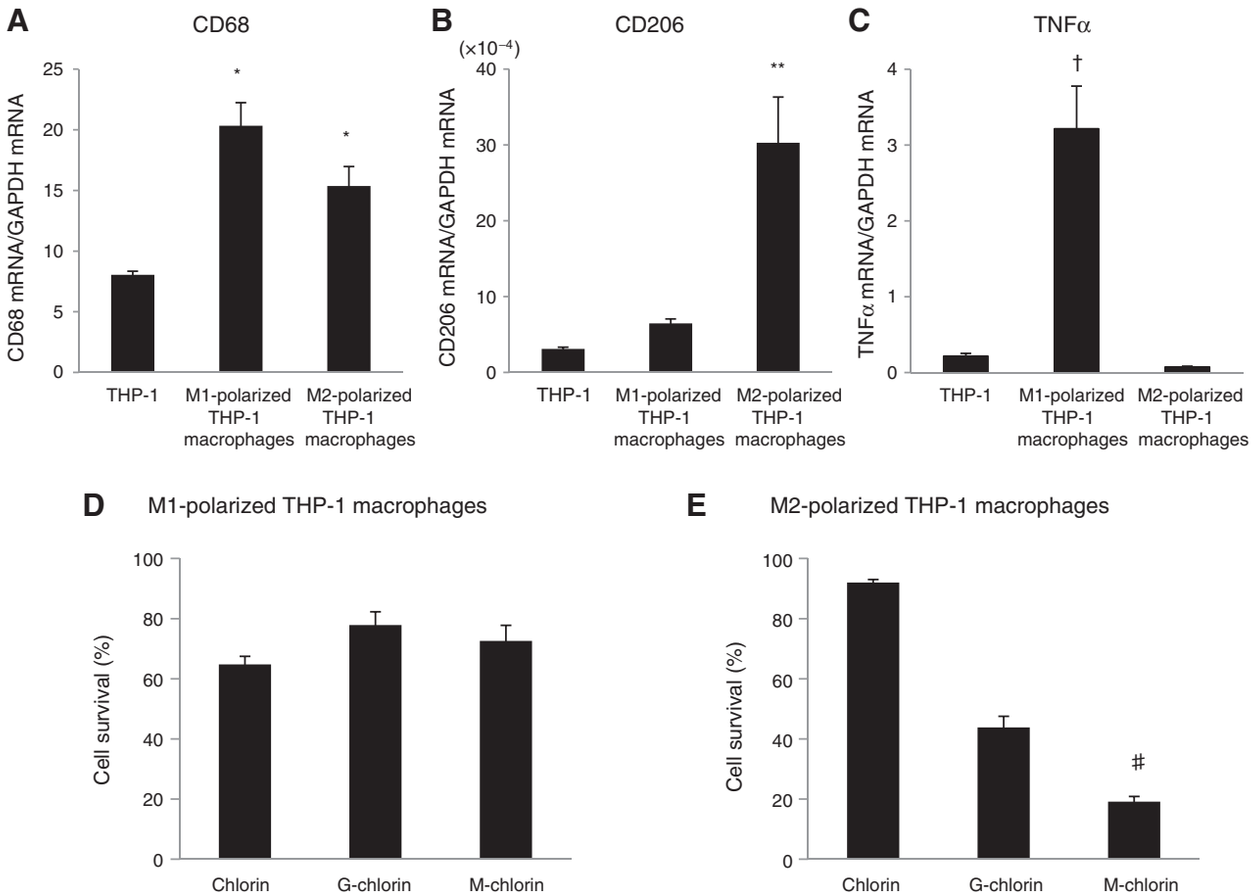


**Figure 4.**

Characterization of THP-1, M1 and M2-polarized THP-1 macrophages, and the effects of PDT with M-chlorin. A, CD68 (marker of macrophages differentiation), B, CD206 (marker of TAMs), and C, TNFα, mRNA expression levels in THP-1 and M1, M2-polarized THP-1 macrophages were evaluated. *, $P < 0.01$, M1, M2-polarized THP-1 macrophages versus THP-1, **, $P < 0.01$, M2-polarized THP-1 macrophages versus THP-1 and M1-polarized THP-1 macrophages; †, $P < 0.0005$, M1-polarized THP-1 macrophages versus THP-1 and M2-polarized THP-1 macrophages, D and E, M1- and M2-polarized THP-1 macrophages were incubated with 1 μmol/L photosensitizer in culture medium for 24 hours, irradiated with 5.6 J/cm$^2$ of 660 nm LED light, and incubated for 24 hours. Cell viability was determined by a WST-8 assay. Data are means of three independent experiments ± SE. #, $P < 0.01$, M-chlorin versus chlorin and G-chlorin.

(CD206) than the THP-1 cells and M1-polarized THP-1 macrophages ($P < 0.01$; Fig. 4B), while TNFα mRNA expression was increased significantly in M1-polarized THP-1 macrophages compared with THP-1 cells and M2-polarized THP-1 macrophages ($P < 0.0005$; Fig. 4C).

Then, we evaluated the M2 macrophage death induced by PDT with M-chlorin. M1, M2-polarized THP-1 macrophages were then loaded with 1 μmol/L photosensitizer (chlorin, G-chlorin, M-chlorin) for 24 hours and irradiated at 5.6 J/cm$^2$. PDT with chlorin, G-chlorin, and M-chlorin was equally effective against M1-polarized macrophages (Fig. 4D), but PDT with M-chlorin induced cell death more effectively in M2 macrophages than PDT with chlorin or G-chlorin (Fig. 4E). These findings revealed that PDT with M-chlorin selectivity induced cell death against M2 macrophages compared with PDT with chlorin or G-chlorin.

### M-chlorin PDT strongly suppressed tumor growth *in vivo*

To examine the effects of M-chlorin PDT on tumors *in vivo*, PDT was performed on allograft models established by subcutaneously implanting mouse colon cancer cells (CT26) into mice models. When tumors grew, mice were given an intraperitoneal injection of photosensitizers, and 24 hours later were irradiated. PDT was performed two times on day 1 and day 8. M-chlorin PDT mediated significantly suppressed tumor growth compared with control treatment, chlorin PDT, and G-chlorin PDT (Fig. 5).

### M-chlorin PDT attacks TAMs

Finally, we analyzed tumors for the selective elimination of TAMs from the tumor stroma after M-chlorin PDT using an anti-F4/80 antibody to stain macrophages and an anti-CD206 (mannose receptor) antibody to stain TAMs (Fig. 6A). Mouse macrophages and TAMs in a 250 × 250 μm area were counted in triplicate and averaged. Both F4/80-positive macrophages and CD206-positive TAMs in the tumor stroma were significantly decreased by M-chlorin and G-chlorin PDT compared with respective numbers in the control and chlorin PDT groups ($P < 0.01$) (Fig. 6B). As shown in Fig. 6C, the ratio of TAMs/macrophages in tumor stroma treated by M-chlorin was significantly decreased compared with those in the control, chlorin, and G-chlorin groups ($P < 0.01$). These results

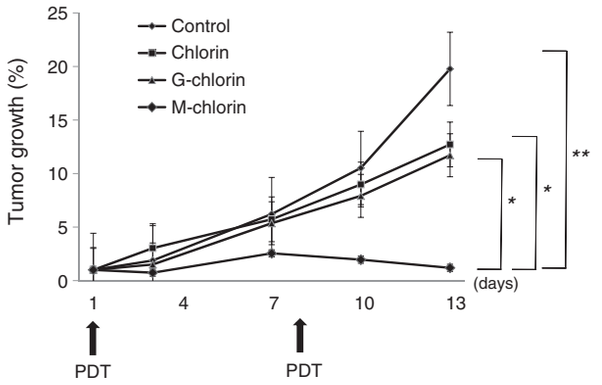


**Figure 5.**
Antitumor effects of PDT in mouse allograft model. Mice were irradiated with 13.9 J/cm$^2$ of LED light at 660 nm 24 hours after injection of the photosensitizer. PDT was performed on day 1 and day 8, and tumor volumes were monitored for 13 days in total. Data are means ± SE ($n = 4$ for control, $n = 5$ for chlorin, G-chlorin, and M-chlorin). *, $P < 0.05$; **, $P < 0.01$.

indicated that PDT with M-chlorin effectively induced cell death against TAMs infiltrated into cancer stroma and that this could explain, at least in part, how M-chlorin PDT induces strong antitumor effects in an allograft model.

## Discussion

Macrophages activated by bacterial products and Th1 cytokines are regarded as M1 macrophages, which are classically activated macrophages with high anti-bacterial activity and cytotoxicity against cancer cells. On the other hand, macrophages activated by Th2 cytokines such as IL4 and IL13 or immune suppressors such as IL10 are classified as M2 macrophages, which have low cytotoxicity, but strong tissue-remodeling activity (1, 7, 8, 26). TAMs are predominantly M2 macrophages induced to accumulate in tumor stroma by chemokines from the cancer cells such as monocyte chemotactic protein-1 (MCP-1), macrophage colony stimulating factor (M-CSF or CSF-1), and VEGF (2, 6–8). TAMs directly promote tumor cell growth by producing growth factors, while both cancer cells and TAMs also produce the immunosuppressive cytokine TGF-β, which effectively blunts the antitumor response by cytotoxic T cells (1, 8), further promoting tumor survival. TAMs also activate neovascularization by producing VEGFs, FGFs, IL17, and IL23, and play a role in proteolytic remodeling of the extracellular matrix (ECM) by producing matrix metalloproteinase (MMP)-9 and urokinase-type plasminogen activator receptor (uPAR); both of these processes are very important for cancer cell invasion and metastases (9, 44).

In this study, we investigated whether M-chlorin could act as a potential photosensitizer for PDT against gastric and colon cancer cells *in vitro* and *in vivo*. G-chlorin was initially developed by linking glucose to the photosensitizer chlorine-based on tumors consuming higher levels of glucose than normal cells and thus G-chlorin providing improved cancer cell targeting than chlorin or other photosensitizers (29, 36). We subsequently produced M-chlorin with the aim of targeting TAMs, which overexpress mannose receptors, but not cancer cells. Indeed, we hypothesized that M-chlorin PDT might not have any effects on cancer cells. To our surprise, PDT with M-chlorin induced cancer cell death *in vitro* with 10 to 40 times more efficacy than chlorin alone, and similarly to G-chlorin PDT.

We therefore analyzed the expression of four mannose receptor family members, mannose receptor (MR), M-type phospholipase $A_2$ receptor ($PLA_2R$), DEC-205/gp200-MR6, and Endo 180/uPARAP by quantitative real-time RT-PCR in gastric and colon cancer cells, and found various expressions levels (Supplementary Fig. S3). We therefore speculated that the cancer cells tested also use mannose receptor family members for endocytosis just like macrophages.

The mannose receptor family is a subgroup of the C-type lectin superfamily and comprises four members: the mannose receptor (MR), the M-type phospholipase $A_2$ receptor ($PLA_2R$), DEC-205/gp200-MR6, and Endo 180/uPARAP (18, 19, 45). These receptors consist of a type I transmembrane receptor with an N-terminal cysteine-rich domain, a single fibronectin type II (FN II) domain, and 8–10 C-type lectin-like domains, and all play crucial roles in endocytosis and phagocytosis by recycling between the plasma membrane and the endosomal apparatus (18). The MR also plays crucial roles in the innate and adaptive immune systems, while the PLA2R can internalize soluble PLA2 enzymes, DEC-205 functions in the internalization of antigen for presentation to T lymphocytes, and Endo180 is involved in remodeling of the ECM (18). Our confocal microscopy studies showed that M-chlorin was mainly localized in lysosomes and ER after PDT in the CT26 cancer cells, consistent with the mannose receptors' important roles in the endocytosis to lysosome pathway. We speculate that M-chlorin may be trapped by mannose receptors and thus trafficked by endocytosis to lysosomes via early and late endosomes.

PDT with M-chlorin induced apoptosis in cancer cells (CT26) with the peak at 4 hours after irradiation. Western blotting of nuclear protein showed that PDT with M-chlorin increased nuclear translocation of Nrf2 gradually from 0.5 hours onward after PDT (Supplementary Fig. S4), indicating ROS generation and subsequent disruption of the Nrf2/Keap1 association, leading to the nuclear translocation of Nrf2.

Although PDT with M-chlorin and G-chlorin were almost equally effective at targeting tumor cells *in vitro*, M-chlorin–mediated PDT *in vivo* significantly suppressed tumor growth than G-chlorin–mediated PDT. In addition, M-chlorin and G-chlorin specifically accumulated on tumor region than chlorin *in vivo* (Supplementary Fig. S5). We therefore speculated that the difference in efficacy between M-chlorin PDT and G-chlorin PDT could lie in the difference of effects against TAMs in tumor stroma. Further investigation of TAMs in the tumor stroma by CD206 fluorescence immunostaining of frozen sections revealed that more M-chlorin tended to accumulate on CD206 expressing TAMs than G-chlorin does (Supplementary Fig. S6). These findings explain the reason why M-chlorin specifically kill the CD-206–expressing TAMs (Fig. 6B and C).

Figure 6 represents the striking change in the observed pattern of F4/80-positive macrophage distribution following PDT with G- and M-chlorin. Both these agents accumulated on F4/80-positive macrophages in the tumor, whereas M-chlorin tended to accumulate on CD206-positive TAMs more specifically than G-chlorin. This could explain why M-chlorin has significantly stronger effects against CD206-positive TAMs compared with G-chlorin (Fig. 6C). Furthermore, M-chlorin PDT was specifically effective against M2-polarized THP-1 macrophages that highly express mannose receptors. We also revealed that excess mannose reduced the binding of M-chlorin to the macrophages and tumor cells in dose-dependent manner (Supplementary Fig. S7). On the

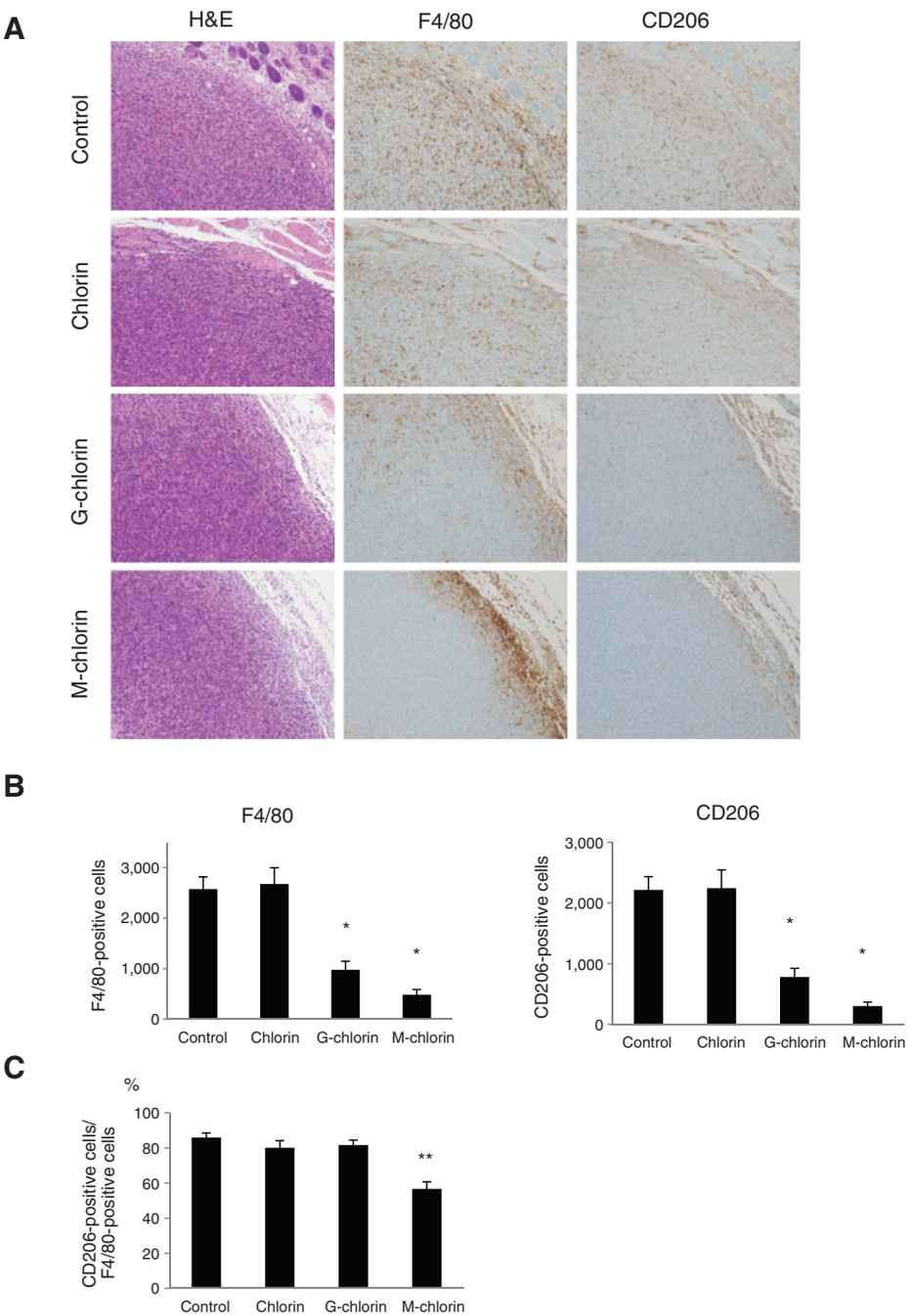


**Figure 6.**
Immunohistochemistry of allograft tumors. Mice were irradiated with 13.9 J/cm$^2$ of LED light at 660 nm 24 hours after injection and then were deeply anesthetized and killed at 3 days after illumination. The tumors were immediately excised and fixed in formalin for immunohistochemical examination. A, the anti-F4/80 antibody was used as a specific marker for macrophages and the anti-CD206 antibody was used as a specific marker for TAMs. Sections were stained with HE (left), anti-F4/80 (middle) antibodies, and anti-CD206 (right) antibodies. Magnification ×100. B, macrophages (F4/80-positive cells) and TAMs (CD206-positive cells) in 250 × 250 μm of tumor images were counted in triplicate. C, the ratio of TAMs to macrophages in tumor filtrates (TAMs/macrophages) from the control, chlorin, G-chlorin, and M-chlorin PDT groups. *, $P < 0.01$, G-chlorin, and M-chlorin versus control; **, $P < 0.01$, M-chlorin versus control, chlorin, and G-chlorin.

basis of these findings, we propose that the cytotoxic effects of M-chlorin PDT on both cancer cells and TAMs expressing high levels of mannose receptor might translate to very strong anticancer effects in an allograft model.

In recent years, many reports showed that TAMs are strongly associated with advanced tumor stage and poor progress in several types of cancer (12, 14, 46). Consequently, therapeutic targeting of TAMs has been proposed for cancer therapy to delay tumor growth (20–22, 25). Mannose receptor is a pathogen recognition receptor and the major receptor responsible for endocytosis in dendritic cells (47). Thus, while M-chlorin may accumulate on the systemic populations of M2 macrophages, the cytotoxic effects of M-chlorin PDT might only affect the tumor microenvironment under irradiation. Peptide therapy or DNA vaccine therapy against M2 macrophages expressing high levels of mannose receptors were reported to be beneficial against cancer (16, 20, 22), but these therapies attack not only TAMs in cancer stroma, but also M2 macrophages throughout the body, risking the induction of immunosuppression. Such a risk would not be an issue with our M-chlorin PDT therapy, which targets only TAMs in tumor stroma and thus should not affect immune responses elsewhere.

In conclusion, we evaluated the anticancer effects of targeting TAMs via PDT with M-chlorin. The specific suppression of TAMs in cancer stroma significantly suppressed tumor growth in allograft models. Such therapeutic targeting of TAMs as well as cancer cells may represent a new strategy for anticancer therapy.

## Disclosure of Potential Conflicts of Interest

No potential conflicts of interest were disclosed.

## Authors' Contributions

**Conception and design:** H. Kataoka, S. Yano
**Development of methodology:** H. Kataoka, M. Tanaka
**Acquisition of data (provided animals, acquired and managed patients, provided facilities, etc.):** H. Kataoka, S. Suzuki, Y. Mori, S. Takahashi
**Analysis and interpretation of data (e.g., statistical analysis, biostatistics, computational analysis):** H. Kataoka, M. Tanaka, S. Suzuki, E. Kubota, S. Tanida
**Administrative, technical, or material support (i.e., reporting or organizing data, constructing databases):** M. Tanaka, E. Kubota, S. Takahashi
**Writing, review, and/or revision of the manuscript:** N. Hayashi, H. Kataoka
**Study supervision:** H. Kataoka, S. Tanida, T. Joh
**Other (preparation of compounds):** K. Moriwaki, H. Akashi

## Acknowledgments

The authors thank Yukimi Ito and Chiaki Koike at Nagoya City University Graduate School of Medical Sciences for technical assistance. The authors also thank Prof. Hideya Yuasa of the Tokyo Institute of Technology for helpful discussions.

## Grant Support

This work was financially supported by JSPS KAKENHI grant number 23590923, JSPS KAKENHI grant number 24790717, JSPS KAKENHI grant number 25288028, JSPS KAKENHI grant number 219350031, JSPS KAKENHI grant number 5288028, the Japan-German Exchange Program supported by the JSPS and the Deutsche Forschungsgemeinschaft, the Hori Sciences and Arts Foundation (2013), Japan Science and Technology Agency A-step (2011), Japan Science and Technology Agency Molecular Imaging (2011, 2012, 2013), and The Japanese Foundation for Research and Promotion of Endoscopy (2011).

The costs of publication of this article were defrayed in part by the payment of page charges. This article must therefore be hereby marked *advertisement* in accordance with 18 U.S.C. Section 1734 solely to indicate this fact.

Received April 22, 2014; revised September 23, 2014; accepted December 4, 2014; published OnlineFirst December 15, 2014.

## References

1. Sica A, Schioppa T, Mantovani A, Allavena P. Tumour-associated macrophages are a distinct M2 polarised population promoting tumour progression: potential targets of anti-cancer therapy. Eur J Cancer 2006;42:717–27.
2. Sica A, Allavena P, Mantovani A. Cancer related inflammation: the macrophage connection. Cancer Lett 2008;267:204–15.
3. Pollard JW. Tumour-educated macrophages promote tumour progression and metastasis. Nat Rev Cancer 2004;4:71–8.
4. Franco OE, Shaw AK, Strand DW, Hayward SW. Cancer associated fibroblasts in cancer pathogenesis. Semin Cell Dev Biol 2010;21:33–9.
5. Xing F, Saidou J, Watabe K. Cancer associated fibroblasts (CAFs) in tumor microenvironment. Front Biosci 2010;15:166–79.
6. Bingle L, Brown NJ, Lewis CE. The role of tumour-associated macrophages in tumour progression: implications for new anticancer therapies. J Pathol 2002;196:254–65.
7. Solinas G, Germano G, Mantovani A, Allavena P. Tumor-associated macrophages (TAM) as major players of the cancer-related inflammation. J Leukoc Biol 2009;86:1065–73.
8. Allavena P, Sica A, Solinas G, Porta C, Mantovani A. The inflammatory micro-environment in tumor progression: the role of tumor-associated macrophages. Crit Rev Oncol Hematol 2008;66:1–9.
9. Qian BZ, Pollard JW. Macrophage diversity enhances tumor progression and metastasis. Cell 2010;141:39–51.
10. Buddingh EP, Kuijjer ML, Duim RA, Burger H, Agelopoulos K, Myklebost O, et al. Tumor-infiltrating macrophages are associated with metastasis suppression in high-grade osteosarcoma: a rationale for treatment with macrophage activating agents. Clin Cancer Res 2011;17:2110–9.
11. Lewis CE, Pollard JW. Distinct role of macrophages in different tumor microenvironments. Cancer Res 2006;66:605–12.
12. Ryder M, Ghossein RA, Ricarte-Filho JC, Knauf JA, Fagin JA. Increased density of tumor-associated macrophages is associated with decreased survival in advanced thyroid cancer. Endocr Relat Cancer 2008;15:1069–74.
13. Zhu P, Baek SH, Bourk EM, Ohgi KA, Garcia-Bassets I, Sanjo H, et al. Macrophage/cancer cell interactions mediate hormone resistance by a nuclear receptor derepression pathway. Cell 2006;124:615–29.
14. Chen JJ, Lin YC, Yao PL, Yuan A, Chen HY, Shun CT, et al. Tumor-associated macrophages: the double-edged sword in cancer progression. J Clin Oncol 2005;23:953–64.
15. Roca H, Varsos ZS, Sud S, Craig MJ, Ying C, Pienta KJ. CCL2 and interleukin-6 promote survival of human CD11b+ peripheral blood mononuclear cells and induce M2-type macrophage polarization. J Biol Chem 2009;284:34342–54.
16. Vasievich EA, Huang L. The suppressive tumor microenvironment: a challenge in cancer immunotherapy. Mol Pharm 2011;8:635–41.
17. Allavena P, Chieppa M, Bianchi G, Solinas G, Fabbri M, Laskarin G, et al. Engagement of the mannose receptor by tumoral mucins activates an immune suppressive phenotype in human tumor-associated macrophages. Clin Dev Immunol 2010;2010:547179.
18. East L, Isacke CM. The mannose receptor family. Biochim Biophys Acta 2002;1572:364–86.
19. Taylor PR, Gordon S, Martinez-Pomares L. The mannose receptor: linking homeostasis and immunity through sugar recognition. Trends Immunol 2005;26:104–10.
20. Luo Y, Zhou H, Krueger J, Kaplan C, Lee SH, Dolman C, et al. Targeting tumor-associated macrophages as a novel strategy against breast cancer. J Clin Invest 2006;116:2132–41.
21. Rao G, Wang H, Li B, Huang L, Xue D, Wang X, et al. Reciprocal interactions between tumor-associated macrophages and CD44-positive cancer cells via osteopontin/CD44 promote tumorigenicity in colorectal cancer. Clin Cancer Res 2013;19:785–97.
22. Cieslewicz M, Tang J, Yu JL, Cao H, Zavaljevski M, Motoyama K, et al. Targeted delivery of proapoptotic peptides to tumor-associated macrophages improves survival. Proc Natl Acad Sci U S A 2013;110:15919–24.
23. Zeisberger SM, Odermatt B, Marty C, Zehnder-Fjallman AH, Ballmer-Hofer K, Schwendener RA. Clodronate-liposome-mediated depletion of tumour-associated macrophages: a new and highly effective antiangiogenic therapy approach. Br J Cancer 2006;95:272–81.
24. Chen P, Huang Y, Bong R, Ding Y, Song N, Wang X, et al. Tumor-associated macrophages promote angiogenesis and melanoma growth via adrenomedullin in a paracrine and autocrine manner. Clin Cancer Res 2011;17:7230–9.
25. Lamagna C, Aurrand-Lions M, Imhof BA. Dual role of macrophages in tumor growth and angiogenesis. J Leukoc Biol 2006;80:705–13.
26. Sica A, Mantovani A. Macrophage plasticity and polarization: in vivo veritas. J Clin Invest 2012;122:787–95.
27. Mroz P, Yaroslavsky A, Kharkwal GB, Hamblin MR. Cell death pathways in photodynamic therapy of cancer. Cancers 2011;3:2516–39.
28. Dolmans DE, Fukumura D, Jain RK. Photodynamic therapy for cancer. Nat Rev Cancer 2003;3:380–7.
29. Yano S, Hirohara S, Obata M, Hagiya Y, Ogura S, Ikeda A, et al. Current states and future views in photodynamic therapy. J Photochem Photobiol C 2011; Photochemistry Reviews 12 (2011) 46–67.
30. Abels C. Targeting of the vascular system of solid tumours by photodynamic therapy (PDT). Photochem Photobiol Sci 2004;3:765–71.

31. Allison RR, Moghissi K. Photodynamic therapy (PDT): PDT mechanisms. Clin Endosc 2013;46:24–9.
32. Li Z, Agharkar P, Chen B. Therapeutic enhancement of vascular-targeted photodynamic therapy by inhibiting proteasomal function. Cancer Lett 2013;339:128–34.
33. Horimatsu T, Muto M, Yoda Y, Yano T, Ezoe Y, Miyamoto S, et al. Tissue damage in the canine normal esophagus by photoactivation with talaporfin sodium (laserphyrin): a preclinical study. PLoS ONE 2012;7:e38308.
34. Dougherty TJ, Cooper MT, Mang TS. Cutaneous phototoxic occurrences in patients receiving Photofrin. Lasers Surg Med 1990;10:485–8.
35. Nelson JS, Roberts WG, Berns MW. In vivo studies on the utilization of mono-L-aspartyl chlorin (NPe6) for photodynamic therapy. Cancer Res 1987;47:4681–5.
36. Tanaka M, Kataoka H, Mabuchi M, Sakuma S, Takahashi S, Tujii R, et al. Anticancer effects of novel photodynamic therapy with glycoconjugated chlorin for gastric and colon cancer. Anticancer Res 2011;31:763–9.
37. Warburg O. On the origin of cancer cells. Science 1956;123:309–14.
38. Palaskas N, Larson SM, Schultz N, Komisopoulou E, Wong J, Rohle D, et al. 18F-fluorodeoxy-glucose positron emission tomography marks MYC-overexpressing human basal-like breast cancers. Cancer Res 2011;71:5164–74.
39. Jadvar H, Alavi A, Gambhir SS. 18F-FDG uptake in lung, breast, and colon cancers: molecular biology correlates and disease characterization. J Nuclear Med 2009;50:1820–7.
40. Fletcher JW, Djulbegovic B, Soares HP, Siegel BA, Lowe VJ, Lyman GH, et al. Recommendations on the use of 18F-FDG PET in oncology. J Nuclear Med 2008;49:480–508.
41. Tanaka M, Kataoka H, Yano S, Ohi H, Moriwaki K, Akashi H, et al. Antitumor effects in gastrointestinal stromal tumors using photodynamic therapy with a novel glucose-conjugated chlorin. Mol Cancer Ther 2014;13:767–75.
42. Hirohara S, Obata M, Alitomo H, Sharyo K, Ando T, Tanihara M, et al. Synthesis, photophysical properties and sugar-dependent in vitro photocytotoxicity of pyrrolidine-fused chlorins bearing S-glycosides. J Photochem Photobiol B Biol 2009;97:22–33.
43. Tjiu JW, Chen JS, Shun CT, Lin SJ, Liao YH, Chu CY, et al. Tumor-associated macrophage-induced invasion and angiogenesis of human basal cell carcinoma cells by cyclooxygenase-2 induction. J Invest Dermatol 2009;129:1016–25.
44. Marconi C, Bianchini F, Mannini A, Mugnai G, Ruggieri S, Calorini L. Tumoral and macrophage uPAR and MMP-9 contribute to the invasiveness of B16 murine melanoma cells. Clin Exp Metastasis 2008;25:225–31.
45. Martinez-Pomares L. The mannose receptor. J Leukoc Biol 2012;92:1177–86.
46. Tsutsui S, Yasuda K, Suzuki K, Tahara K, Higashi H, Era S. Macrophage infiltration and its prognostic implications in breast cancer: the relationship with VEGF expression and microvessel density. Oncol Rep 2005;14:425–31.
47. Sallusto F, Cella M, Danieli C, Lanzavecchia A. Dendritic cells use macropinocytosis and the mannose receptor to concentrate macromolecules in the major histocompatibility complex class II compartment: downregulation by cytokines and bacterial products. J Exp Med 1995;182:389–400.